Supplementary Figures:

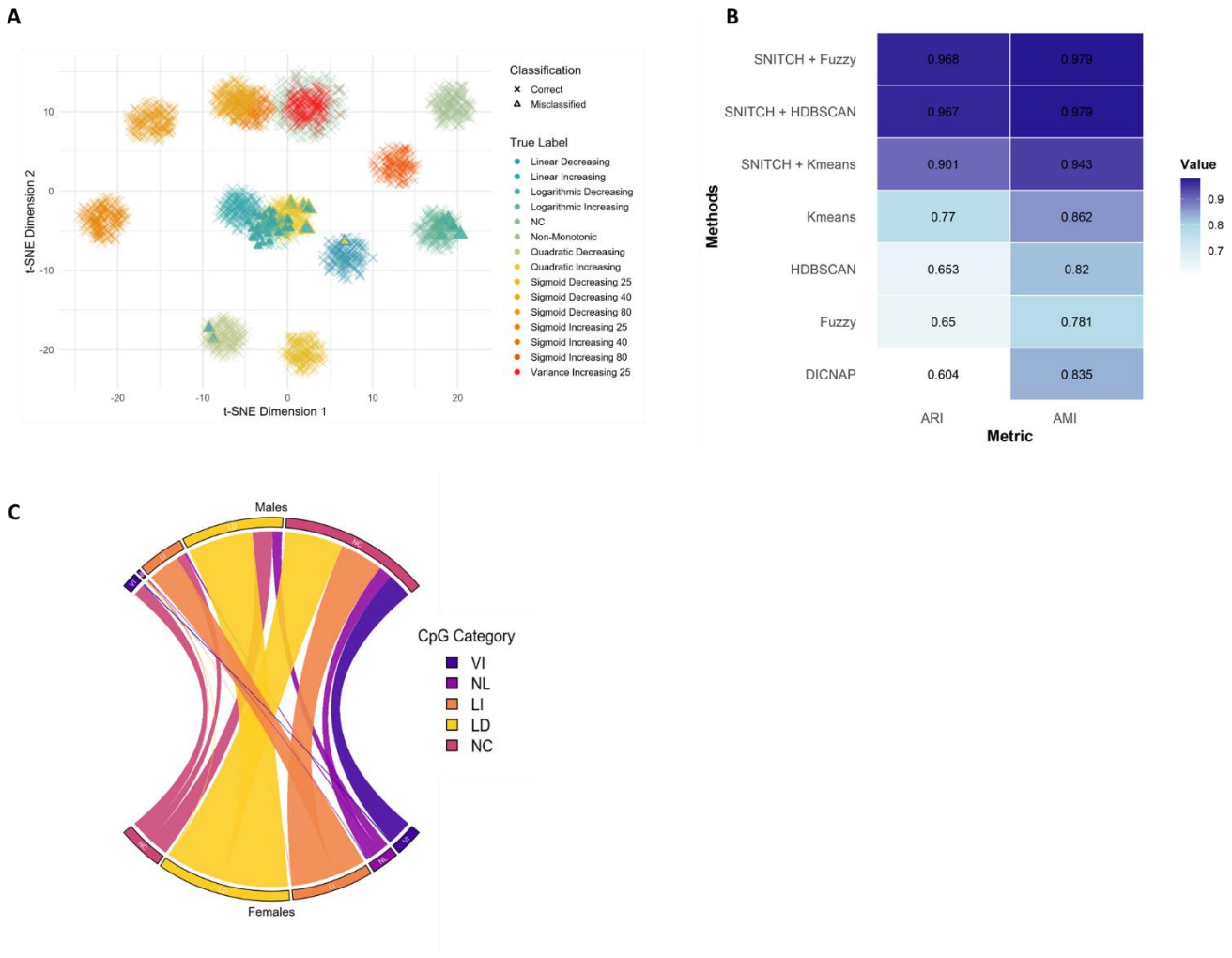

Supp. Figure 1: **A**, T-SNE representation of the simulated CpGs to illustrate their true and assigned labels after SNITCH. **B**, Benchmark of SNITCH compared to stand-alone unsupervised clustering methods and DICNAP. **C**, Conserved CpGs between male and female clusters.

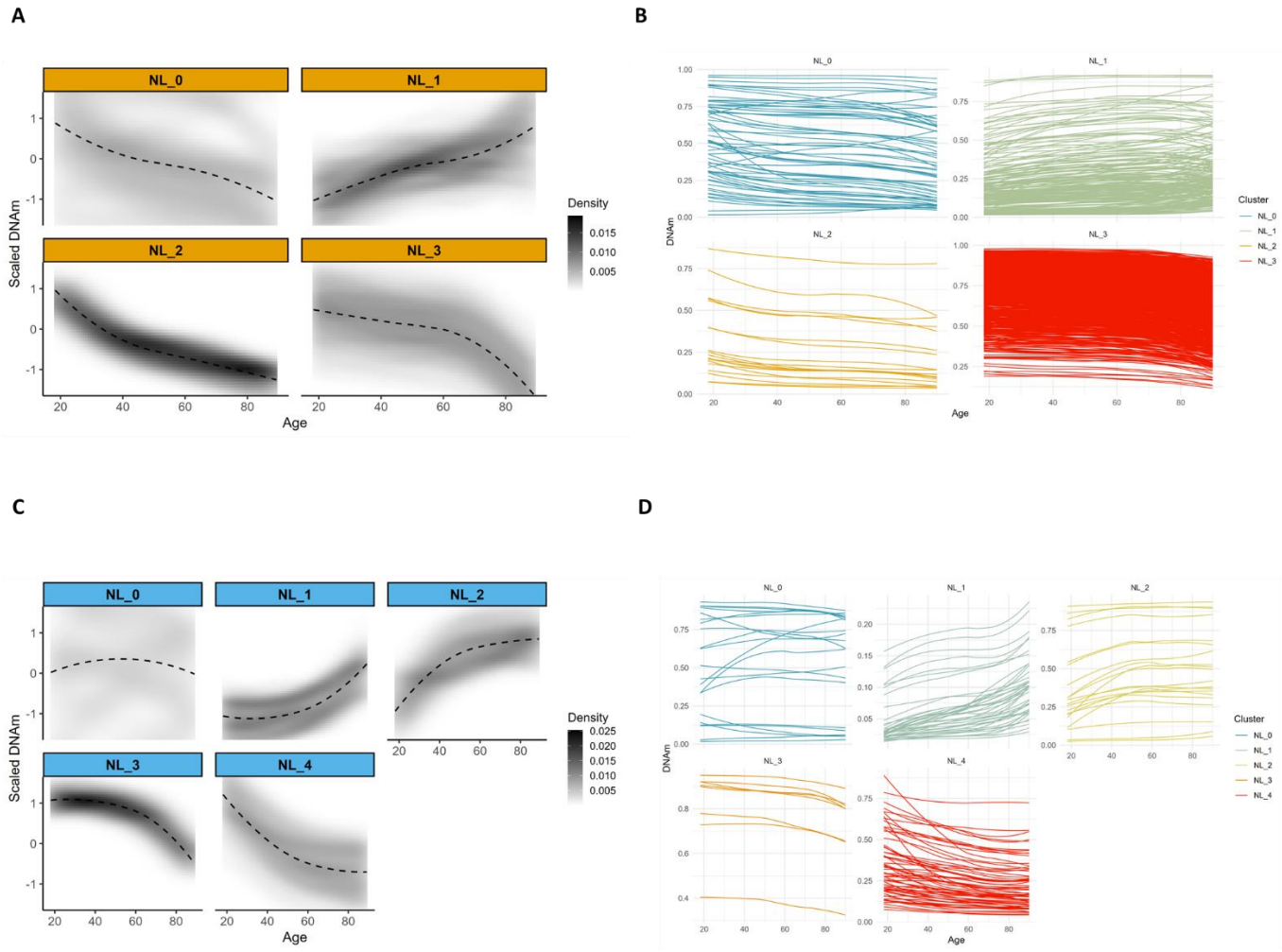

Supp. Figure 2: **A**, Initial non-linear clusters identified in females. Beta values were centered and scaled prior to FPCA and unsupervised clustering and are used to better illustrate the patterns. **B**, Unscaled beta values in the initial females' non-linear clusters. : **C**, Initial non-linear clusters identified in males. Beta values were centered and scaled prior to FPCA and unsupervised clustering and are used to better illustrate the patterns. **B**, Unscaled beta values in the males' initial non-linear clusters.

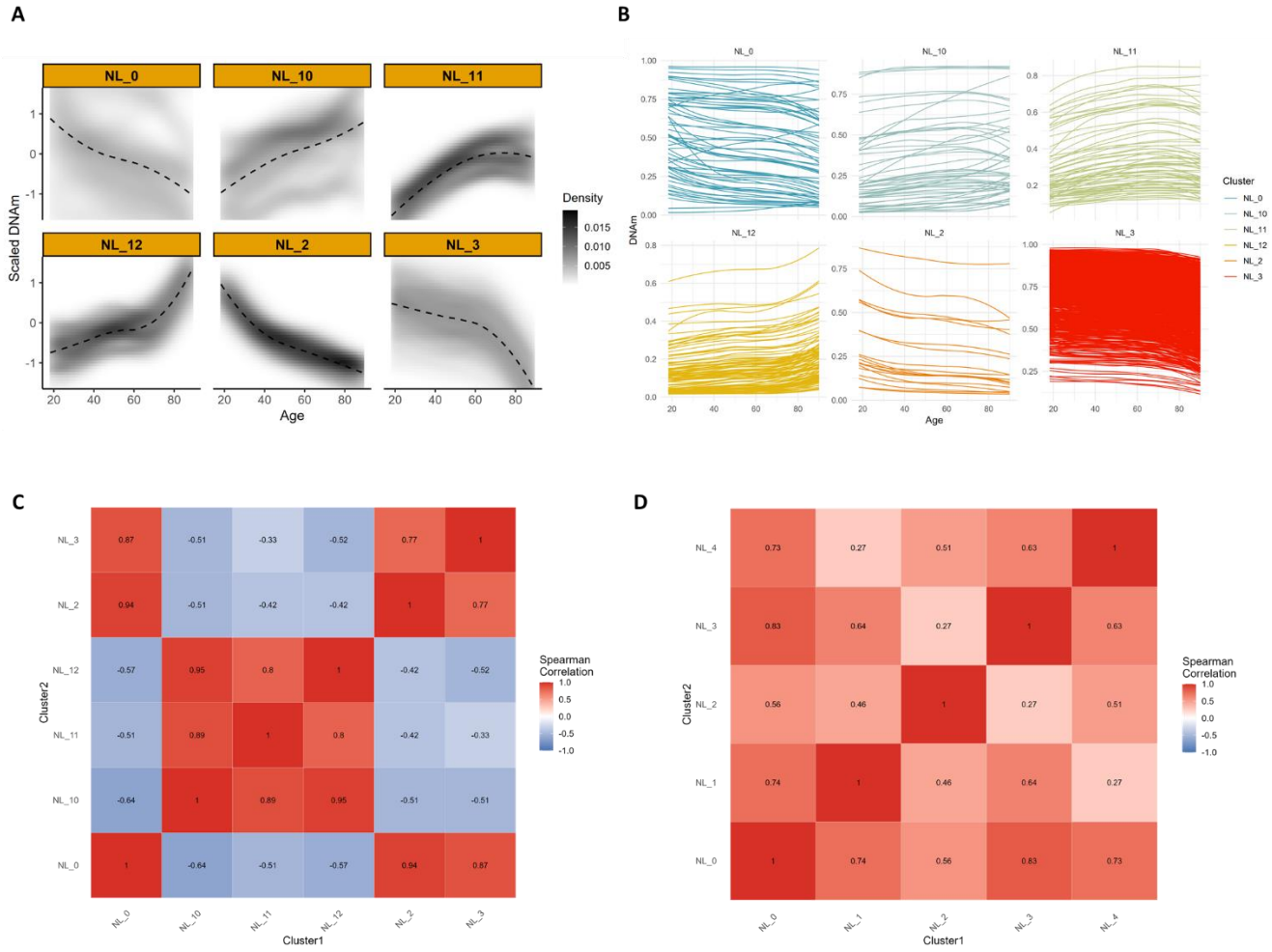

Supp. Figure 3: **A**, Non-linear clusters identified in females after the reclassification of NL1. Beta values were centered and scaled prior FPCA and unsupervised clustering and are used to better illustrate the patterns. **B**, Unscaled beta values in the females' non-linear clusters after the reclassification of NL1. **C**, Correlation matrix between the NL clusters eigenvalues in females. **D**, Correlation matrix between the NL clusters eigenvalues in males.

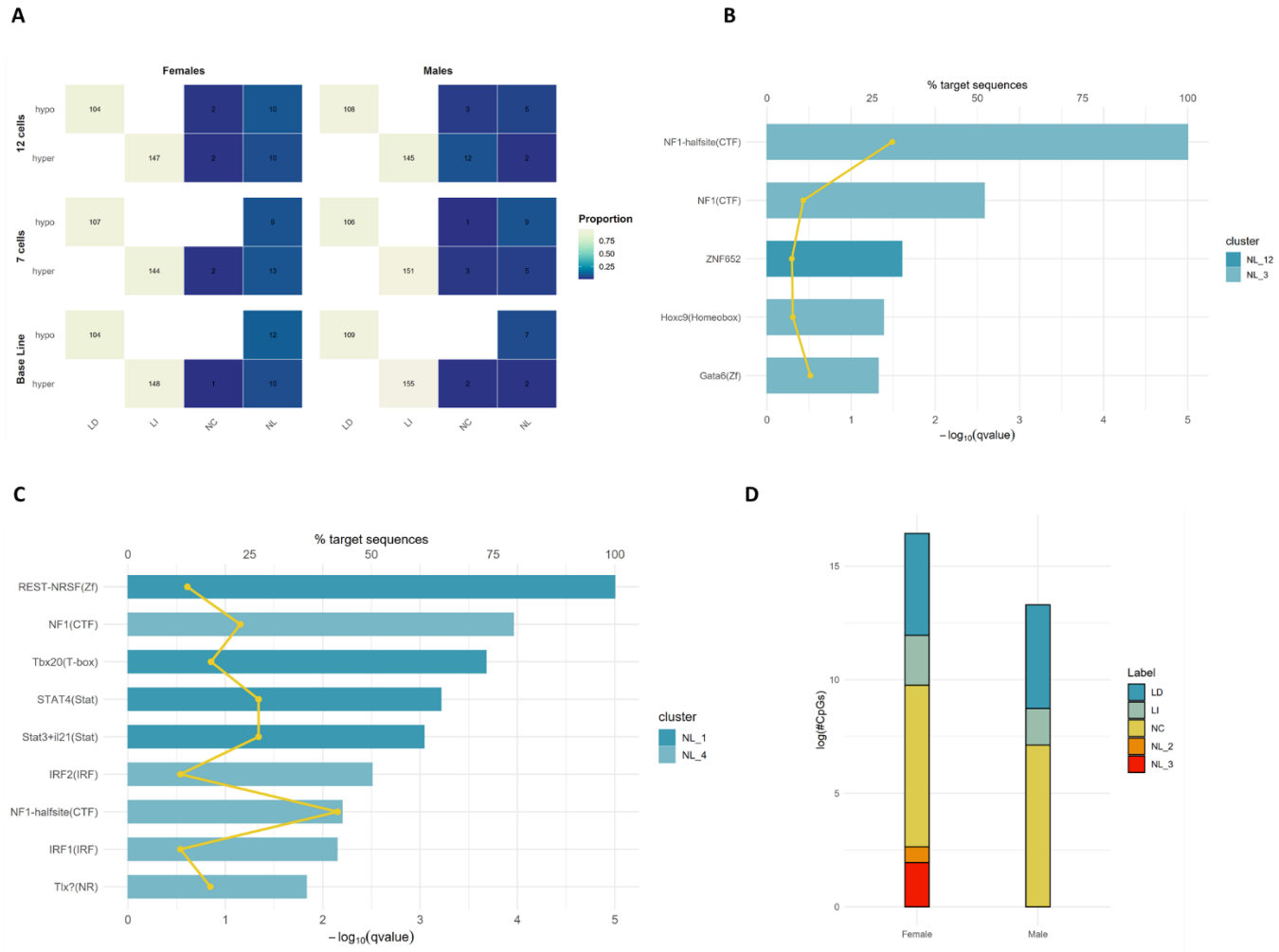

Supp. Figure 4: **A**, Enrichment of CpG labels across age-CpGs identified in the EWAS study by Roy R. et al.. **B**, Cluster-wise motif enrichment analysis among females NL CpGs. **C**, Cluster-wise motif enrichment analysis among females NL CpGs. **D**, Distribution of the CpGs used to estimate C-Reactive Protein levels among males and females aging classification.

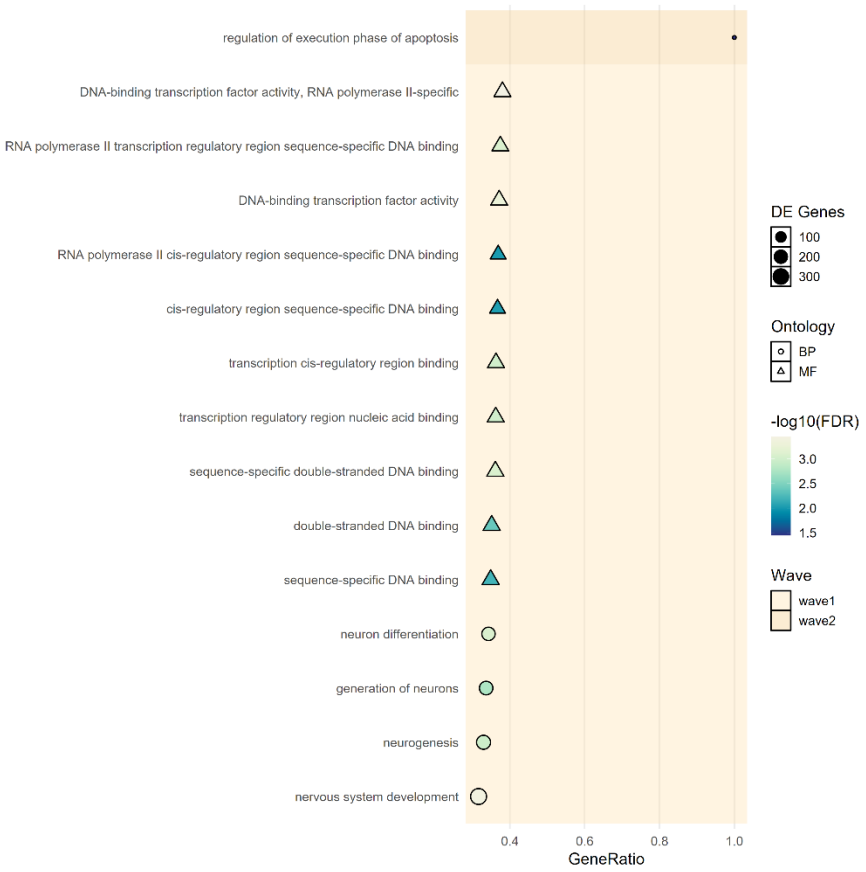

Supp. Figure 5: Pathway enrichment analysis performed among common CpGs identified across waves of dysregulation in females.